OPEN ACCESS
IOP Publishing
Plasma Sources Science and Technology
Plasma Sources Sci. Technol. **29** (2020) 095022 (8pp)
https://doi.org/10.1088/1361-6595/abb0d1

# Interface reactions between water and ionic wind generated by d.c. corona discharge in nitrogen

**Zhongshu Zhang, Mark P Wilson, Scott J MacGregor, Igor V Timoshkin, Martin Given and Tao Wang***

Department of Electronic and Electrical Engineering, University of Strathclyde, Royal College Building, 204 George Street, Glasgow, United Kingdom, G1 1XW

E-mail: tao.wang@strath.ac.uk

Received 26 September 2019, revised 29 July 2020
Accepted for publication 19 August 2020
Published 28 September 2020

**Abstract**

This work investigated the interface reactions between water and ionic wind from a positive d.c. corona discharge in nitrogen. The effects of drift ions and active neutral species were investigated on their production of hydrogen peroxide in water. Both positive drift ions and active neutral species were found to produce hydrogen peroxide in water. 1 mol positive drift ions can produce 0.13 mol hydrogen peroxide under atmospheric pressure; a reduced gas pressure increased the production of hydrogen peroxide, with 1 mol ions producing 0.29 mol hydrogen peroxide at 100 torr. The gas pressure has little effect on the production of hydrogen peroxide by active neutral species. The drift positive ions acted as ion anode on water surface, reacting with water to produce hydrogen, oxygen, and hydrogen peroxide. The adsorbed form of OH and O produced at the interface can synergistically work to react with the OH scavengers in water. Both $HO_2$ and $H_2O_2$ from the discharge were transported to water to produce the liquid phase hydrogen peroxide.

Keywords: corona discharge, plasma, hydroxyl radicals, hydrogen peroxide, ionic wind, ion anode

(Some figures may appear in colour only in the online journal)

## 1. Introduction

The interactions between water and plasma have been studied for more than two hundred years since the first report by Cavendish's in 1785. In recent researches, the interfacial processes between plasma and liquid have been deeply investigated, which include the processes caused by neutral species, ions, electrons and plasma electrochemistry. At the plasma–liquid interface, neutral species such as O, $O_3$, OH, NO, $HO_2$, $H_2O_2$, $HNO_2$ and $HNO_3$ from the discharge can be transported to the liquid (Bruggemann *et al* 2016). Sano investigated the interface reactions between water and corona discharges in $N_2/O_2$, and found that the neutral species like oxygen atom was generated in the presence of oxygen, and then carried by ionic wind to the water surface, producing aqueous hydroxyl radicals (Sano *et al* 2002).

The reactions of energetic positive ions at the plasma–liquid interface was also investigated. The atomic simulations have shown that 100 eV $O_2^+$ can penetrate to 3 nm below the liquid surface (Nikiforov 2008). Water molecules can be sputtered to the gas phase after impinged by the energised ions (Minagawa *et al* 2014). Energised ions bombard the water surface to excite, ionize or dissociate the water molecules, and produce hydroxyl radicals, which have short lifetime of 2.7 $\mu$s at the interface (Attri *et al* 2015). The kinetic energy of positive ions bombarding the water cathode causes $H_2O$ excitation and ionization, and eventually

* Author to whom any correspondence should be addressed.



 

dissociation to protons and hydroxyl radicals (Cserfalvi and Mezei 1996). The plasma induced electrochemical process at the interface has been proved able to exceed the 100% current efficiency by Faraday's law based upon the stoichiometry of the given electrochemical reactions. Hickling investigated contact glow discharge electrolysis, and found that the hydrogen peroxide produced in the electrolyte can reach 1.8 times the predicted by Faraday's law at 760 torr; the hydrogen peroxide formation was thought due to the positive ions accelerated through the cathode fall entering the liquid and dissociating water molecules (Hickling and Ingram 1964). Sengupta analysed the chemical yields of contact glow discharge electrolysis, and found that water molecule dissociation partly occurred in the plasma near anode to produce $H_2$ and $O_2$, and in anolyte to produce $H_2$, $O_2$ and $H_2O_2$ (Sengupta and Singh 1994). Kanzaki believed that $H_2O^+$ was produced in gas phase in anode glow discharge electrolysis (Kanzaki *et al* 1986). In plasma electrolysis, one electron can participate in multiple reactions in gas phase, which increased the current efficiency. The energised electrons can excite, ionize or dissociate water molecules at the interface; non-energised electrons transported to liquid eventually become solvated electrons, which can recombine with cations or react with water molecules to produce hydroxide ions and hydrogen. Locke *et al* reviewed the energy yield of hydrogen peroxide production for various plasma-water interface reactions; most results obtained were between 0–1 g $kWh^{-1}$ (Locke and Shih 2011). The low energy yield limits the application of plasma-induced advanced oxidation processes for water purification.

For a water cathode glow discharge, the average kinetic energy of positive ions entering the water was suggested to be greater than 100 eV (Sengupta *et al* 1998). The mean kinetic energy of drift ions, produced by corona discharge, reaching the water surface is only 0.01–0.1 eV (Chen and Davidson 2003). There have been few investigations of the reactions between positive drift ions and liquid water. In the present study, the mechanisms of positive drift ions and active neutral species from the corona discharge in nitrogen were evaluated in their ability to produce hydrogen peroxide in water. The effects of gas pressure, flow rate and the interface reaction mechanisms were investigated.

## 2. Experimental set-up

### 2.1. Electrical circuit

The experimental layout is shown in figure 1(a). Corona discharges were generated using needle electrodes, charged by a Glassman, PS/EJ20R30 d.c. power supply. The current limiting resistors are $R_1$ and $R_2$; the current-viewing resistor is $R_3$. $R_2$ has a large resistance of 24.9 M$\Omega$, which ensures the current is d.c. without pulses and protect the probe on $R_3$ once pulse current occurred. The voltage applied to the needle electrode was measured by a Tektronix P6015A high voltage probe. The gap voltage from needle to cathode was calculated by subtracting the partial voltage across $R_2$ (which equals to 747 V at 30 $\mu$A d.c. current) from the needle voltage measured by the high voltage probe. The voltage on the CVR was measured by a Teledyne LeCroy PP008 probe. Both voltage waveforms were recorded using a Teledyne LeCroy Waverunner 610Zi oscilloscope.

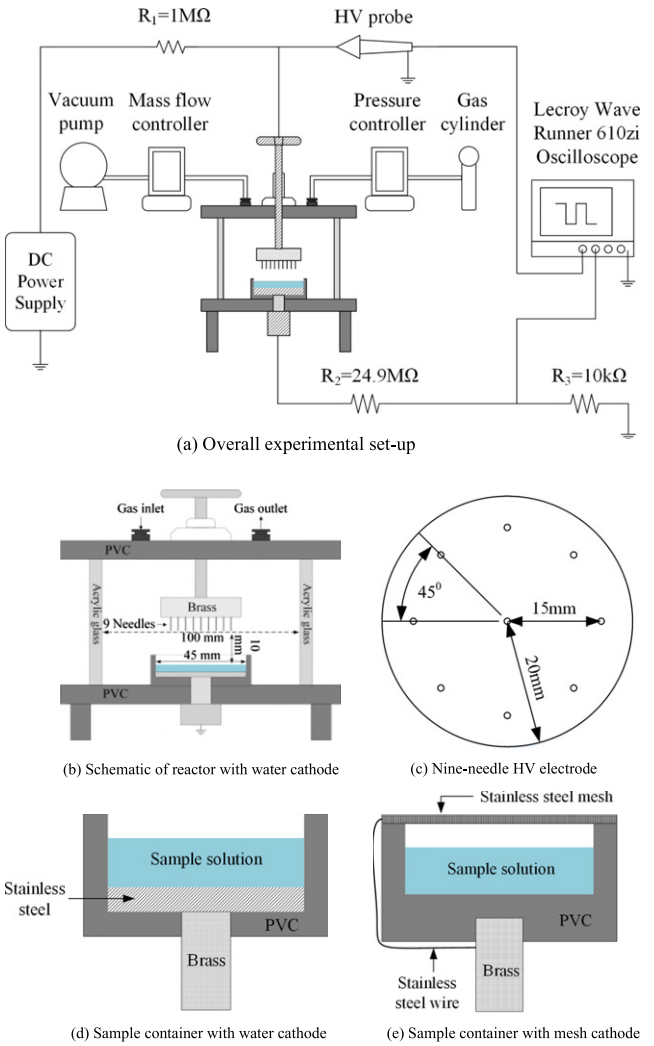


**Figure 1.** Experimental set-up and reactor configurations.

### 2.2. Reactor design

The chamber of the gas-sealed reactor encompassed an acrylic tube, with an inner diameter of 100 mm and a height of 100 mm. The gas inlet and outlet ports were situated on the lid. The tip radius of the needles was 0.2 mm. Inside the reactor, either a water cathode or a stainless-steel mesh cathode was used in the experiment. For experiments with water cathode, positive corona discharges were generated between a nine-needle high-voltage (HV) electrode and the sample solution. The gap between the needle tips and the solution surface was fixed at 10 mm. The solution was grounded through a stainless-steel plate at the bottom of the container, as illustrated in figure 1(d).

For experiments with mesh cathode, positive corona discharge was generated between the nine-needle HV electrode and the grounded mesh. The mesh was placed 5.3 mm above the solution surface, covering the entire surface. The gap

between the needle tips and the mesh was 10 mm. The positive ions were filtered by the mesh, allowing only neutral species to reach the solution. The mesh pore size was 1 mm, and the wire diameter was 0.3 mm. The thickness of the mesh was 0.6 mm.

### 2.3. Gas preparation

For each experiment, the reactor was vacuumed to lower than 4 torr and refilled with flowing nitrogen. The process was repeated three times. The gas pressure was measured and controlled using an upstream pressure controller Alicat Scientific PC-30PSIA-D/5P, with a range of 0–1500 torr absolute, a resolution of 1 torr, and accuracy of 0.25%. The gas flow rate was set within the range of 0–10 slpm using an Alicat Scientific MC-10SLPM-D/5M mass flow controller, with a resolution of 0.01 slpm, and accuracy of 0.8%. The flow mass controller was put at the downstream side of the reactor to coordinate with the upstream pressure controller to set the working gas pressure and flow rate.

### 2.4. Sample preparation and experimental procedures

Three types of sample solutions were prepared for use in the experiments: deionized water; 0.1 mol $l^{-1}$ tert-butanol (TB) solution; and 0.1 mol $l^{-1}$ dimethyl sulfoxide (DMSO) solution. Deionized water, with a conductivity lower than 1 $\mu$S $cm^{-1}$, was prepared using a Milli-Q Integral 15 water purification system. The 0.1 mol $l^{-1}$ TB solution was made by introducing 0.19 ml of TB (ACS reagent, $\geqslant$99.7%, CAS 75-65-0, Sigma-Aldrich) to 19.81 ml of deionized water, via a 1 ml pipette (Gilson, P1000G). The 0.1 mol $l^{-1}$ DMSO solution was made by introducing 0.14 ml of DMSO (ACS reagent, $\geqslant$99.9%, CAS 67-68-5, Sigma-Aldrich) to 19.86 ml of deionized water via a 1 ml pipette (Gilson, P1000G).

The concentration of $H_2O_2$ was measured via spectrophotometric determination with potassium titanium (IV) oxalate ($K_2TiO(C_2O_4)_2$). Two different solutions were used: 0.1 mol $l^{-1}$ $Ti^{4+}$ solution; and 1 mol $l^{-1}$ $H_2SO_4$ solution. The 0.1 mol $l^{-1}$ $Ti^{4+}$ solution was prepared by dissolving 3.54 g $K_2TiO(C_2O_4)_2$ (Technical, $\geqslant$90%, Ti basis, Sigma-Aldrich) into 100 ml of deionized water. The 1 mol $l^{-1}$ $H_2SO_4$ was prepared by diluting 5.36 ml of concentrated sulphuric acid (AR reagent, >95.0%, CAS 7664-93-9, Fisher Scientific) in 94.64 ml of deionized water.

For the tests using deionized water, 5 ml deionized water was transferred into the sample container, via a 5 ml pipette (Gilson, P5000G). For the tests using TB solution or DMSO solution, 4.5 ml of deionized water was transferred into the sample container. Then, 0.5 ml of 0.1 mol $l^{-1}$ TB solution or DMSO solution was added to achieve a concentration of 0.01 mol $l^{-1}$.

The $H_2O_2$ produced in the solution was measured immediately after the exposure to the ionic wind generated by the corona discharge. Firstly, 3 ml of treated solution was mixed with 0.3 ml of 0.1 mol $l^{-1}$ $Ti^{4+}$ solution and 0.3 ml of 1 mol $l^{-1}$ sulfuric acid solution. The peroxotitanium complex $Ti(O_2)OH(H_2O)_3$ was formed in the solution, exhibiting a yellow colour and peak absorption at 390 nm, measured using a Thermo Scientific Evolution 201 spectrophotometer. The absorption and hydrogen peroxide concentration measurements were calibrated against a reference solution of $H_2O_2$ with known concentration.

To measure pH and conductivity, 3 ml of treated solution was mixed with 12 ml of deionized water immediately after each test. The solution pH was measured with a Thermo Scientific Orion Star A211 pH metre, and the conductivity was measured with a Thermo Scientific Orion Star A325 pH/conductivity metre. The results were converted to the pre-dilution values.

The concentration of nitrite and nitrate in the solution was measured by a colorimetric test kit (Sigma-Aldrich, Cat. No. 11746081001). The nitrite reacts with sulfanilamide and N-(1-naphthyl)-ethylene-diamine dihydrochloride to form a diazo dye, exhibiting a red colour and peak absorbance at 540 nm which can be measured by a spectrophotometer. The treated samples were divided into two groups, in one group the nitrite is measured; in the other group, the nitrate was reduced to nitrite by nicotinamide adenine dinucleotide phosphate in the presence of the enzyme nitrate reductase, and the total nitrite was measured. By comparing the difference of nitrite concentration, the nitrate concentration can be determined. Three independent experiments were conducted for each test under the same experimental conditions and procedures to ensure the results are reproducible. The mean value was used as the data point on the graph with the uncertainty displayed in standard deviations. The uncertainty in this work mainly comes from the instability of the corona discharge; though the corona current was kept constant at 30 $\mu$A for all the experiments, the needle voltage and the electric field distribution might vary for each experiment.

## 3. Experimental results

### 3.1. Corona discharge characteristics

The corona current was kept constant at 30 $\mu$A using the nine-needle electrode. No pulse current was observed when measuring the current with a matched, 50 Ω coaxial cable. The discharge power at atmospheric pressure was 240 mW for water cathode and 200 mW for mesh cathode. At 100 torr, the discharge power decreased to 93 mW for water cathode and 97 mW for mesh cathode. The corona discharge was also tested with a single-needle electrode, but the d.c. current could not reach 30 $\mu$A without causing large current pulses.

### 3.2. $H_2O_2$ production in water

The $H_2O_2$ production increased linearly with increasing treatment time for tests with both water cathode and mesh cathode. Higher gas flow rate would decrease the concentration of both active neutral species and water vapour in the reactor. Figure 2 illustrates $H_2O_2$ production with gas flow rates of 0.002 slpm, 0.02 slpm and 1.0 slpm at atmospheric pressure.

As figure 2 shows, $H_2O_2$ production decreased when the gas flow rate increased from 0.002 slpm to 1.0 slpm for both types of cathodes. The rate of decline of $H_2O_2$ production with increasing gas flow rate was significant with the mesh cathode,

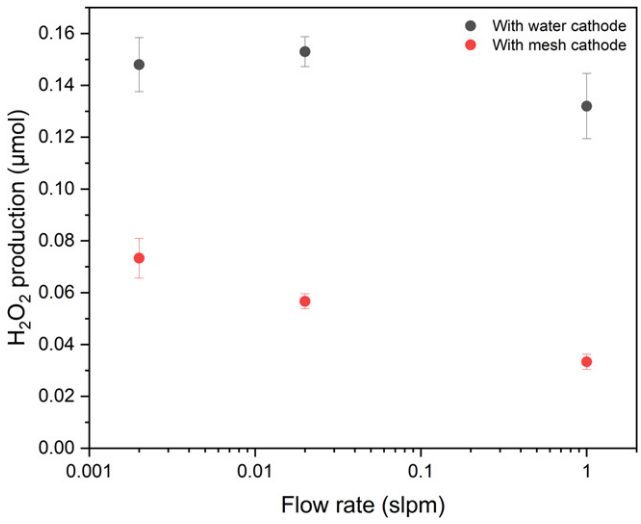


**Figure 2.** $H_2O_2$ production in deionized water following 30 min corona discharge with various gas flow rates at atmospheric pressure. The average d.c. corona current was 30 $\mu$A.

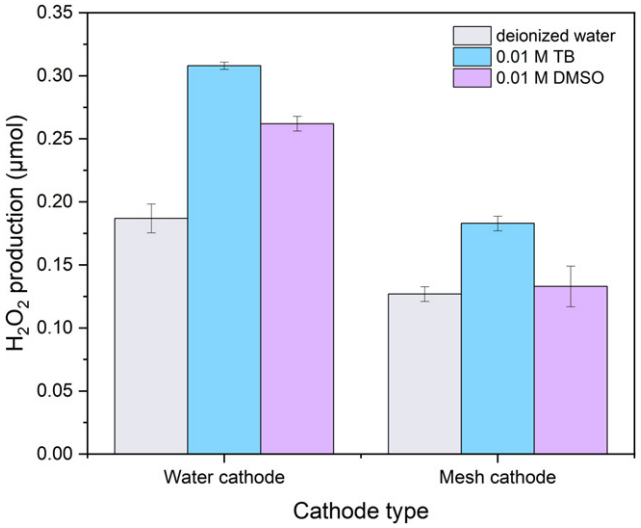


**Figure 3.** $H_2O_2$ production in deionized water, TB and DMSO solution following 30 min corona discharge in nitrogen. Gas pressure was 300 torr and gas flow rate was 0.5 slpm. The average d.c. corona current was 30 $\mu$A.

where the positive ions were filtered. At 0.002 slpm and atmospheric pressure, the contribution of active neutral species to $H_2O_2$ production was around 50%, dropping to around 25% at 1.0 slpm.

A two-layer mesh cathode was tested in order to verify the ionic wind reduction by the mesh. In the two-layer mesh tests, two meshes were both grounded and placed above the solution surface. The gap between the two meshes was set to 1 mm. The distance from the lower layer to the solution surface was 5.3 mm. The needle tip was 10 mm above the upper mesh. The production of hydrogen peroxide was found to be the same as that with a single-layer mesh cathode. The influence of the mesh pore size was also explored, and there was no significant difference in the production of hydrogen peroxide between mesh cathodes with pore sizes of 1 mm and 10 mm. These results suggested that the mesh did not affect the flow of active neutral species to the solution surface. The results prove that the difference in $H_2O_2$ production between the water and mesh cathode was mainly caused by the positive drift ions that were filtered by the mesh.

Increased distance between the mesh and solution was found to reduce the effect of active neutral species on hydrogen peroxide production. $H_2O_2$ production decreased by 43.3% when the distance was increased to 33.3 mm; when a squared PTFE disk (with thickness of 1 mm and side length of 60 mm) was situated beneath the mesh covering the whole mesh area, with a distance of 33.3 mm to the water surface, the hydrogen peroxide production was reduced by 90%. The PTFE disk blocked the transportation of active neutral species into the solution.

### 3.3. OH or $H_2O_2$ produced?

To investigate the reaction path for hydrogen peroxide formation in the solution, and whether this is via the dimerization of hydroxyl radicals, two types of OH scavengers were used in the experiment: TB (tert $-$ $C_4H_9OH$) and DMSO ($(CH_3)_2SO$).

If the $H_2O_2$ in the solution was from dimerization of OH, the addition of TB or DMSO would scavenge OH and reduce the $H_2O_2$ production. The reactions between OH and these two scavengers are:

$$OH + \text{tert} - C_4H_9OH \rightarrow CH_2C(CH_3)_2OH + H_2O \quad (1)$$

$$OH + (CH_3)_2SO \rightarrow (CH_3)_2SO(OH) \quad (2)$$

Three sample solutions were tested: deionized water, 0.01 mol $l^{-1}$ TB solution, and 0.01 mol $l^{-1}$ DMSO solution. Each sample was treated for 30 min at a gas pressure of 300 torr and a gas flow rate of 0.5 slpm. In the tests with TB solution at 760 torr, the corona discharge current could not reach 30 $\mu$A without causing pulses. When the gas pressure was reduced to 300 torr, the corona discharge current could maintain at 30 $\mu$A.

In the water cathode tests, $H_2O_2$ production increased by 64.7% and 40.1% with the addition of TB and DMSO, as figure 3 shows.

In the mesh cathode tests, only active neutral species reached the solution. Hydrogen peroxide production increased by 43.5% with the addition of TB, while the addition of DMSO had minimal effect on $H_2O_2$ production.

The OH scavengers did not reduce the $H_2O_2$ production, implying that neither positive drift ions nor active neutral species acted to produce OH in the solution. Higher concentrations (0.05 mol $l^{-1}$ and 0.1 mol $l^{-1}$) of TB and DMSO solution were used, but identical results were obtained. The $H_2O_2$ in the solution was possibly transported from the gas phase ($H_2O_{2(g)}$ $\rightarrow$ ($H_2O_{2(aq)}$).

### 3.4. pH and conductivity

Five millilitres of deionized water were treated for 60 min with a gas flow rate of 0.2 slpm, at 760 torr. The original conductivity of the deionized water was measured to be 0.75 $\mu$S $cm^{-1}$. After treatment, the conductivity increased to

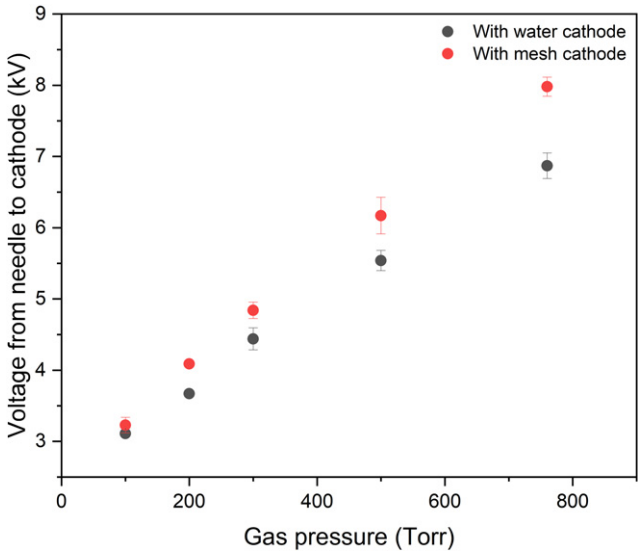


**Figure 4.** Variation of gap voltage with gas pressure with 30 $\mu$A d.c. current at a gas flow rate of 0.002 slpm.

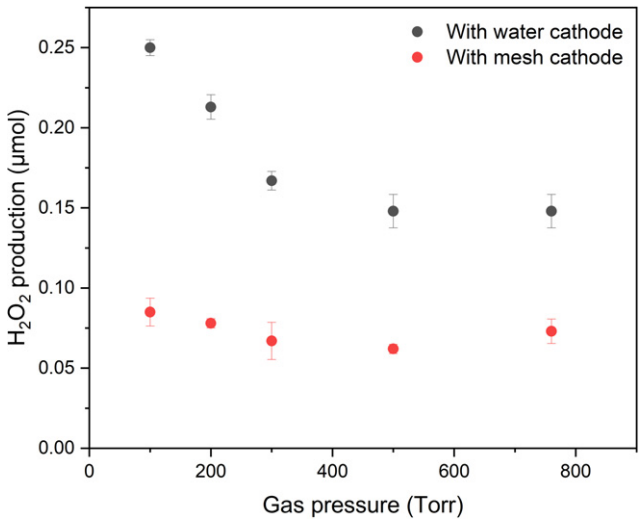


**Figure 5.** Variation of $H_2O_2$ production in deionized water with gas pressure following 30 min corona discharge in nitrogen, at a gas flow rate of 0.002 slpm. The average d.c. corona current was 30 $\mu$A.

38.0 $\mu$S cm$^{-1}$ and 41.3 $\mu$S cm$^{-1}$ for the water cathode tests and mesh cathode tests, respectively. The original pH of the deionized water was around 6.40. The pH of the treated water was 4.38 following tests with the water cathode, and 4.60 for the mesh cathode. The conductivity and pH of the treated deionized water for the two types of cathode are very close, indicating that the active neutral species led to the change of conductivity and pH in water. With water cathode, the concentration of $NO_2^-$ and $NO_3^-$ was measured to be 0.035 mmol l$^{-1}$ and 0.123 mmol l$^{-1}$; with mesh cathode, the concentration of $NO_2^-$ and $NO_3^-$ was 0.043 mmol l$^{-1}$ and 0.137 mmol l$^{-1}$. The pH calculated based upon the concentration of $NO_2^-$ and $NO_3^-$ is 3.80 for the water cathode tests and 3.74 for the mesh cathode tests, which proves that the decrease of pH was mainly caused by the production of nitrite and nitrate. Cadorin *et al* also found that the pH of water dropped to 3 following the treatment with corona discharge in nitrogen (Cadorin *et al* 2015). Takahashi *et al* also reported that $NO_2^-$ and $NO_3^-$ were produced in water after plasma treatment in a $N_2/O_2$ gas mixture (Takahashi *et al* 2016).

### 3.5. Gas pressure effect on $H_2O_2$ production

As the gas pressure was reduced, the gap voltage required to maintain a constant 30 $\mu$A d.c. current decreased, as shown in figure 4. The gap voltage from needle to cathode was calculated by subtracting the partial voltage across $R_2$ (which equals to 747 V at 30 $\mu$A d.c. current) from the needle voltage measured by the high voltage probe. The gap voltage with mesh cathode is higher than that of water cathode under the same gas pressure. Since the mesh thickness is 0.6 mm, the practical discharge gap could be larger than 10 mm for mesh cathode. The water resistance is approximately 20 k$\Omega$ at a conductivity of 1 $\mu$S cm$^{-1}$. Since the current was 30 $\mu$A, the partial voltage across the water was around 600 mV at the beginning of gas discharge. As the gas discharge proceeded, the water conductivity increased and the partial voltage dropped. At 100 torr, the gap voltage for the two cathode types was similar. As the gas pressure was raised, the voltage difference between two cathode types also increased, reaching a maximum of 1.11 kV at the highest tested pressure of 760 torr.

The relationship between $H_2O_2$ production and gas pressure was investigated under five different pressures of 100, 200, 300, 500 and 760 torr, as shown in figure 5. Five millilitres of deionized water was treated by positive ionic wind for 30 min, at a gas flow rate of 0.002 slpm.

With water cathode, $H_2O_2$ production was 0.148 $\mu$mol at both 760 torr and 500 torr. As gas pressure was decreased, the $H_2O_2$ production increased, reaching a maximum of 0.250 $\mu$mol at 100 torr. $H_2O_2$ was produced in water by both the positive drift ions and active neutral species from the corona discharge.

With mesh cathode, only active neutral species reacted with water to produce $H_2O_2$. $H_2O_2$ production was much lower than that using the water cathode. The gas pressure did not significantly change $H_2O_2$ production, only a slight increase was found between 500 and 100 torr, with a maximum of 0.085 $\mu$mol obtained at 100 torr.

The difference in $H_2O_2$ production was caused by positive drift ions. The increase of $H_2O_2$ production with the deionized water cathode was mainly contributed by positive drift ions as the gas pressure dropped. When the gas pressure dropped from 760 to 100 torr, the average reduced electric field increased by 3 times approximately, resulting in the positive drift ions attaining higher kinetic energy. As figure 6 shows, the energy efficiency of $H_2O_2$ production increased as gas pressure decreased.

## 4. Discussion

### 4.1. Effect of drift ions

In the gas phase, the concentration of water vapour is much higher than that of positive nitrogen ions. The positive nitrogen

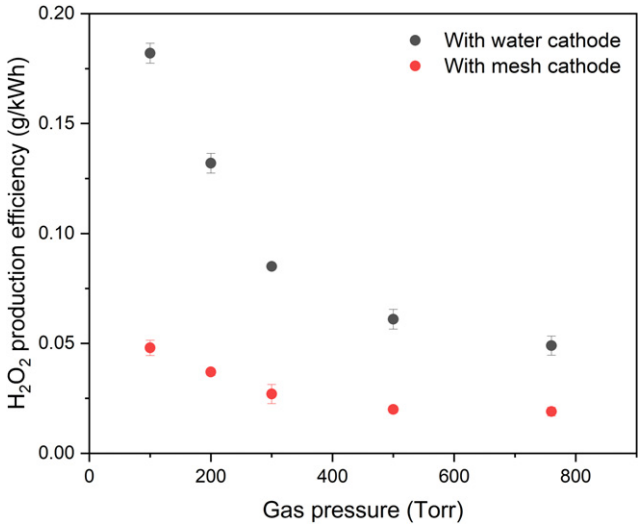


**Figure 6.** Variation of energy efficiency of $H_2O_2$ production with gas pressure following 30 min corona discharge in nitrogen at a gas flow rate of 0.002 slpm. The average d.c. corona current was 30 $\mu$A.

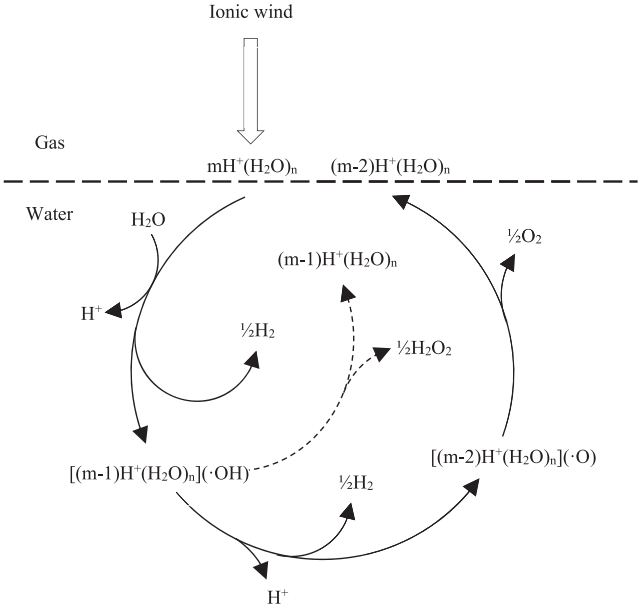


**Figure 7.** Interface reactions of positive drift ions $mH^+(H_2O)_n$ as the ion anode. $m$ is the number of $H^+(H_2O)_n$.

ions would react with water vapour in tens of microseconds (Good *et al* 1970):

$$N_2^+ + H_2O \rightarrow H_2O_g^+ + N_2 \quad (3)$$

Gas-phase water ions $H_2O_g^+$ continue to react with water molecules:

$$H_2O_g^+ + H_2O \rightarrow H_3O^+ + OH \quad (4)$$

The produced OH in reaction (4) would be consumed quickly by self-quenching or reacting with nitrogen compounds in the gas. The hydronium ions $H_3O^+$ continue clustering reactions, and form hydrated hydronium cluster ions $H^+(H_2O)_n$. Good demonstrated that almost all of the positive ions are transformed to $H^+(H_2O)_n$ after 1 ms of discharge in nitrogen containing traces of water vapour (Good *et al* 1970). The formed $H^+(H_2O)_n$ clusters are driven towards the water under the electric field force. The positive ions that eventually reach the water surface are $H^+(H_2O)_n$ clusters. The interface reactions between the positive ions and water also involve electrochemical processes, with bulk of positive drift ions $mH^+(H_2O)_n$ [$m$ is the number of positive drift ions $H^+(H_2O)_n$] acting as the ion anode on water surface.

It has been reported that hydroxyl radicals (OH) and active oxygen (O) can be adsorbed on anode surface in traditional electrolysis with specific electrode materials like Boron-doped diamond and Ti/$SnO_2$ (Marselli *et al* 2003, Comninellis 1994), which is possibly similar to the effect of the ion anode in this case. These electrode materials are non-reactive and have weak adsorption to OH, leading to low $O_2$ evolution but high OH production (Marselli *et al* 2003). The adsorbed hydroxyl radicals M(OH) and oxygen M(O) can form $H_2O_2$ or oxidize organic pollutants in the water (Martı´nez-Huitle and Ferro 2006).

Figure 7 illustrates the possible interface reactions between water and the positive ions $mH^+(H_2O)_n$. $m$ is the number of the positive ions, and $mH^+(H_2O)_n$ acted as the ion anode on water surface. One water molecule loses an electron to the ion anode, producing one $H^+$ and one adsorbed (OH). The ion anode turned into $[(m-1)H^+(H_2O)_n](OH)$. The adsorbed (OH) may self-combine to produce $H_2O_2$, or continue to lose another one electron to the ion anode and produce another $H^+$ and one adsorbed (O), with the ion anode turning into $[(m-2)H^+(H_2O)_n](O)$. The adsorbed (O) can form $O_2$. In this research, one mol positive ions can produce only 0.13 mol hydrogen peroxide in water at atmospheric pressure, and the ratio increased to 0.29 when the gas pressure decreased to 100 torr, suggesting that the production of $H_2O_2$ was concomitant with $O_2$ evolution.

**Table 1.** $H_2O_2$ production by drift ions and active neutral species following 30 min corona discharge at 300 torr with gas flow rate of 0.5 slpm in the deionized water, 0.01 M TB solution and 0.01 M DMSO solution.

| $H_2O_2$ (μmol) | Deionized water | 0.01 M TB | 0.01 M DMSO |
|---|---|---|---|
| Ions | 0.064 | 0.125 | 0.129 |
| Neutral species | 0.123 | 0.183 | 0.133 |
| Total | 0.187 | 0.308 | 0.262 |

The hydrogen peroxide production by ions was doubled when TB or DMSO was added as table 1 presents. No free radicals produced by the plasma–water reactions were found able to react with both TB and DMSO to produce $H_2O_2$. One hypothesis is that the adsorbed hydroxyl radicals $H^+(H_2O)_n(OH)$ and active oxygen $H^+(H_2O)_n(O)$ can synergistically interact with TB and DMSO, doubling the production of hydrogen peroxide.

The mechanisms of $H_2O_2$ formation in the plasma–water interactions have been widely investigated. The hydrogen peroxide production was thought mainly from the dimerization of hydroxyl radicals in gas phase and transported to liquid water,

as in the gliding arc discharge (Locke and Thagard 2009):

$$OH + OH + M \rightarrow H_2O_2 + M \quad (5)$$

The hydroxyl radicals are produced in gas phase by the water dissociation as a result of interactions with electrons, ions and metastables (Fridman 2008, Shainsky *et al* 2012, Locke and Shih 2011, Locke and Thagard 2012):

$$e + H_2O \rightarrow H + OH + e \quad (6)$$

$$e + H_2O \rightarrow H^- + OH \quad (7)$$

$$M^+ + H_2O \rightarrow H_2O^+ + M \quad (8)$$

$$M^+ + H_2O \rightarrow H_2O^* + M^+ \quad (9)$$

$$OH + H_2O^* \rightarrow H_2O_2 + H \quad (10)$$

$$H_2O^+ + H_2O \rightarrow H^+(H_2O) + OH \quad (11)$$

On the other hand, at the plasma–water interface, the kinetic ions can excite and ionize water molecules to produce OH (Bruggeman *et al* 2009), and form hydrogen peroxide in the water. Zhao *et al* investigated the production of hydrogen peroxide in water using pulsed positive discharges in nitrogen with a pin anode and water cathode, and found that the production of hydrogen peroxide decreased significantly with the addition of OH scavenger to water. The decrease of hydrogen peroxide demonstrates that OH is the precursor of hydrogen peroxide, where the interface reactions were initiated by kinetic positive ions (Zhao *et al* 2016). In contact glow discharge electrolysis, the kinetic ions contributed more OH production than the charge-transfer process, resulting in that the current efficiency of $H_2O_2$ production exceeded 100% (Hickling and Ingram 1964). The optical emission spectroscopy also shows there are O, $H_\alpha$ and OH produced in gas phase for a pulsed plasma generated in atmospheric pressure air between a pin anode and a tap water cathode (Bruggeman *et al* 2009).The recombination of electrons with $H_2O^+$ or $H_3O^+$ was thought important in the production of OH.

In this research, the addition of OH scavengers increased the production of hydrogen peroxide, which proves that hydroxyl radicals are not the major reactive products in the reactions between water and positive drift ions.

The drift ions have little kinetic energy, which makes the interface reactions different from the reactions discussed above, and more like an anode process in the electrolysis. The drift ions on water surface break water molecules into the adsorbed (OH) as shown in figure 7, rather than the water excitation and ionization by kinetic ions.

### *4.2. Effects of active neutral species*

In this research, with the addition of TB, the production of $H_2O_2$ by active neutral species was increased by 50%; with the addition of DMSO, the production of $H_2O_2$ was almost unchanged. $HO_2$ was probably the major active neutral species, since it can react with TB to produce $H_2O_2$, and does not react with DMSO.

$$HO_2 + \text{tert} - C_4H_9OH \rightarrow (CH_3)2C(OH)CH_2 + H_2O_2 \quad (12)$$

The self-reaction of $HO_2$ in aqueous phase can generate $H_2O_2$:

$$HO_2 + HO_2 + H_2O \rightarrow H_2O_2 + O_2 + H_2O \quad (13)$$

According to reaction (13), two $HO_2$ can self-react to produce one $H_2O_2$ in water. When TB was added in water, one $HO_2$ can produce one $H_2O_2$. With the same amount of $HO_2$, the addition of TB should double the $H_2O_2$ production. In considering that the total $H_2O_2$ production was increased only by approximately 50% when TB was added, $HO_2$ self-reaction cannot be the only path for $H_2O_2$ production, there should be transportation and dissolution of $H_2O_2$ into the solution, formed via OH dimerization in gas phase (Herron and Green 2001):

$$H_2O^* + H_2O \rightarrow H + OH + H_2O \quad (14)$$

$$N_2(A) + H_2O \rightarrow H + OH + N_2(X) \quad (15)$$

$$N(^2D) + H_2O \rightarrow OH + NH \quad (16)$$

## 5. Conclusions

The research demonstrated that $H_2O_2$ is produced in water under exposure to the ionic wind from d.c. corona discharge in nitrogen. The hydrated hydronium drift ions $H^+(H_2O)$ play an important role at the interface reactions with water. These drift ions act as ion anodes, on which the adsorbed hydroxyl radicals (OH) and adsorbed oxygen (O) are formed, capable of initiating advanced oxidation process in water, accompanying the evolution of oxygen and hydrogen gas, and the formation of $H_2O_2$ in water.

The production of $H_2O_2$ in water was linear with treatment time but affected by gas pressure and flow rate, with 1 mol ions producing 0.29 mol $H_2O_2$ at 100 torr, equivalent to 47 eV in producing one $H_2O_2$ molecule, or an energy yield of 27 g $kWh^{-1}$. The overall energy efficiency was still low in considering that the input energy was mostly dissipated in corona discharge.

The active neutral species that led to the production of $H_2O_2$ in water is thought to be from the combination of $HO_2$ as well as the dissolution of gas phase $H_2O_2$. The water pH and conductivity changes observed following the interactions with the ionic wind were mainly caused by the neutral species, which produced nitrite and nitrate ions in water.

## Acknowledgments

The authors wish to thank Dr Leonard Berlouis for his advice on the mechanisms of interface reactions, and Christopher Jones for his contribution to chemical procedures and test. This research was supported by the REN Plasma Laboratory in University of Strathclyde.

## ORCID iDs

Zhongshu Zhang https://orcid.org/0000-0003-4279-0234

## References


Fridman A 2008 *Plasma Chemistry* (Cambridge: Cambridge University Press)

Attri P *et al* 2015 *Sci. Rep.* **5** 9332

Bruggeman P J *et al* 2016 *Plasma Sources Sci. Technol.* **25** 053002

Bruggeman P *et al* 2009 *Plasma Sources Sci. Technol.* **18** 045023

Cadorin B M *et al* 2015 *J. Hazard. Mater.* **300** 754–64

Chen J and Davidson J H 2003 *Plasma Chem. Plasma Process.* **23** 83–102

Comninellis C 1994 *Electrochim. Acta* **39** 1857–62

Cserfalvi T and Mezei P 1996 *Anal. Bioanal. Chem.* **355** 813–9

Good A, Durden D A and Kebarle P 1970 *J. Chem. Phys.* **52** 212–21

Herron J T and Green D S 2001 *Plasma Chem. Plasma Process.* **21** 459–81

Hickling A and Ingram M D 1964 *Trans. Faraday Soc.* **60** 783–93

Kanzaki Y, Hirabe M and Matsumoto O 1986 *J. Electrochem. Soc.* **133** 2267–70

Locke B R and Shih K-Y 2011 *Plasma Sources Sci. Technol.* **20** 034006

Locke B R and Thagard S M 2009 *IEEE Trans. Plasma Sci.* **37** 494–501

Locke B R and Thagard S M 2012 *Plasma Chem. Plasma Process.* **32** 875–917

Marselli B, Garcia-Gomez J, Michaud P-A, Rodrigo M A and Comninellis C 2003 *J. Electrochem. Soc.* **150** D79–83

Martı´nez-Huitle C A and Ferro S 2006 *Chem. Soc. Rev.* **35** 1324–40

Minagawa Y, Shirai N, Uchida S and Tochikubo F 2014 *Japan J. Appl. Phys.* **53** 010210

Nikiforov A Y 2008 *High Energy Chem.* **42** 235–9

Sano N, Kawashima T, Fujikawa J, Fujimoto T, Kitai T, Kanki T and Toyoda A 2002 *Ind. Eng. Chem. Res.* **41** 5906–11

Sengupta S K and Singh O P 1994 *J. Electroanal. Chem.* **369** 113–20

Sengupta S K, Singh R and Srivastava A K 1998 *Indian J. Chem.* **37A** 558–60

Takahashi K, Satoh K, Itoh H, Kawaguchi H, Timoshkin I, Given M and MacGregor S 2016 *Japan J. Appl. Phys.* **55** 15030

Zhao Y Y, Wang T, Wilson M P, MacGregor S J, Timoshkin I V and Ren Q C 2016 *IEEE Trans. Plasma Sci.* **44** 2084–91